

Heat Transfer Characteristics of a Fluid Flow in Multi Tube Heat Exchanger Fitted with Perforated Fins

Assist. Prof. Dr.Nabil Jamil Yasin
Technical Collage of Baghdad
Middle Technical University
Nabiljamil58@yahoo.com

Dr.Dhia Al-Deen Hussain Alwan
Dhia716@yahoo.co.uk

Ayad Dawood Suliman
ayaddawood89@yahoo.com

ABSTRACT

The heat transfer and flow resistance characteristics for air flow cross over circular finned tube heat exchanger has been studied numerically and experimentally. The purpose of the study was to improve the heat transfer characteristics of an annular finned-tube heat exchanger for better performance. The study has concentrated on the effect of the number of perforations and perforations shapes on the heat transfer and pressure drop across a staggered finned tube heat exchanger. The Numerical part of present study has been performed using ANSYS Fluent 14.5 using SST Turbulent model, while the experimental study consist from a test rig with different models of heat exchangers and all required measurement devices were building up to cover the experimental work for the range of Reynolds number (7500-17500). The experimental results show that average Nusselt number of the six circular perforations fins model is about 11.08 % higher than that for solid fin model and with triangular perforations model is about 10.12 % higher than that for the solid fin. Triangular perforation finned heat exchanger model gives a best result than the other models due to excessive increment in the (Nu) in comparison with other models take in consideration pressure drop. The results were validated with previous work and the comparison between the experimental and numerical shows a good agreement with a maximum deviation $\pm 10\%$ between them.

Key words: Heat Transfer, Heat Exchanger, Perforated Fins.

خصائص انتقال الحرارة لمائع يجري خلال مبادل حراري متعدد الانابيب مجهز بزعانف مثقبة

ايداد داود سليمان

د. ضياء الدين حسين علوان

أ.م.د. نبيل جميل ياسين

الكلية التقنية الهندسية / الجامعة التقنية الوسطى

الخلاصة

تمت دراسة خصائص انتقال الحرارة ومقاومة الجريان للهواء المار عبر مبادل حراري مزعنف نظرياً وتجريبياً. الغرض من هذه الدراسة هو محاولة تحسين خصائص انتقال الحرارة لمنظومة انابيب حلقيه الزعانف للحصول على اداء افضل. ركزت الدراسة على معرفة تأثير عدد الثقوب واشكالها على عملية انتقال الحرارة وانخفاض الضغط خلال مبادل حراري من النوع المتخالف الترتيب. في الدراسة النظرية تم انشاء الشبكة باستخدام برنامج ANSYS Fluent.14 مع موديل الجريان الاضطرابي SST بينما تضمن العملي ضمن ال بناء جهاز تجريبي يحتوي كافة نماذج المبادل الحراري المصنعة وجميع اجهزة القياس المطلوبة لغرض الدراسة التجريبية ضمن حدود عدد رينولد (7500-17500). اظهرت النتائج التجريبية ان عدد نسلت للزعانف الحاوية على ستة ثقوب دائرية اعلى بحدود 11.08% من الزعانف الغير مثقبة. في حين ان عدد نسلت كان اعلى بمقدار 10.12% للزعانف الحاوية على اربع ثقوب مثلثية عن الزعانف الغير مثقبة. كذلك اظهرت الدراسة ان نتائج الزعانف ذوات الثقوب المثلثة هي الافضل بالمقارنة مع باقي النماذج نظراً للزيادة الملحوظة في عدد نسلت بالاخذ بنظر

الاعتبار الزيادة في انخفاض الضغط. تمت مقارنة النتائج النظرية مع بحوث سابقة وكذلك اجريت مقارنة بين النتائج النظرية والتجريبية وقد اظهرت تقارباً مقبولاً بينهما بانحراف لا يتعدى $\pm 10\%$.

الكلمات الرئيسية: انتقال حرارة, مبادل حراري, زعانف مثقبة.

1. INTRODUCTION

Saving material and energy are critical problems for optimization for all aspects of the economy. One of the important issues that should be defined during the design of a heat exchanger, is taking into account the cost of material, and the optimization of the heat efficiency, **Shah 1981**.

A circular finned tube has been widely utilized due to its low manufacturing cost. The fin industry has been engaged with continuous researches to reduce the fin size, weight and cost. The reduction in fin size and cost is achieved by the enhancement of heat transfer that carried out by the fins. This enhancement can be accomplished by different methods such as increasing the ratio of the heat transfer surface area of the fin to its volume, manufacturing fins from materials having high thermal conductivity, and increasing the heat transfer coefficient between the fin and its surroundings, **Incropera 1996**. Fins as a heat transfer enhancement devices must be designed to achieve maximum heat removal with minimum material expenditure, but taking into account the ease of manufacturing of the fin shape. Several studies have introduced some shape modifications by cutting some material from the fin to make cavities, holes, slots, grooves, or perforations through the fin body in order to increase the effective heat transfer surface area and/or the heat transfer coefficient, **Kim, 2008**. The fin industry has been engaged in continuous researches, which deals with perforation fin and other passive and active methods, to reduce the fin size, weight, and cost as well as more heat transfer rate **Prasad, and Gupta, 1998**. Many investigations have studied various geometric shapes of the fins, such as plate fins, circular fins and helical fins, and the benefit of using perforation. **Fayed et al. 2008**, presented an experimental study on the effect of fin's perforation on the thermal performance of helically finned tubes. From the comparison, the overall heat transfer coefficient is found to be increase (12.3%) at air velocity of (4.5m/s) in case of perforated fin, this percentage continued in increasing until to attaining (36%) at (7.5 m/s). **Karabacak and Yakar, 2011**, investigated experimentally the effect of perforations placed on finned tube heat exchangers on convection heat transfer. It was found that Nusselt number increase by adding perforations. **Banerjee et al. 2012**, studied numerically an annular finned-tube array with perforations to assessing the enhancement of heat transfer while minimizing an increase in pressure drop across the domain. It

was found that for the perforated case the heat flux, and heat transfer coefficient performance ratios of the fin increased by 5.96% and 7.07%, respectively.

Ismail, 2013, studied the effects of perforations on the thermal and fluid dynamic performance of a heat exchanger by using different types of perforated shapes having same surface area. A comparison of various geometric configurations showed that the thermal performance of perforated fin is better than that of solid fin.

Most of the studies concentrate on the flat plate fin. Very few articles studied the case of the annular perforated fins numerically and experimentally. The aim of the present work is to study the influence of using the annular perforated fin on the heat transfer process for the flow within a multi tube heat exchanger (numerically and experimentally). Moreover the effect of a number of variables such as number of perforations, diameter of perforation holes, and the effect of perforations shape will be determined numerically using one of the available CFD package and support by an experimental study.

2. CFD MODELING AND SIMULATION

Numerical calculations have been conducted by simulating three-dimensional air flow and heat transfer over solid and perforated finned-tube configurations. The CFD modeling, simulation and post processing have been carried out in an ANSYS 14.5, Workbench environment with an ANSYS system of fluid flow (Fluent).

2.1 The Geometry

A three dimensional finned tube heat exchanger has been simulated by using AutoCAD software and preparation for simulation by using ANSYS Design Modeler software. The numerical study has been performed by taking a section from the full case, because there is no enough computer memory and speed available to fulfill the full case. This section consist of three fins for each pipe. The study includes five cases of heat exchangers according to the types of fins as follows, solid fins, two perforated fins with circular perforation having different numbers of perforations, and finally two perforated fins having square and triangular perforation shapes with same cross section area (19.71 mm^2). **Fig.1** shows all above described cases, and the applied boundary conditions while **Table. 1** shows the description of the five models. The governing equations solved for the flow field are the continuity (mass conservation), Navier-Stokes equations of

motion (momentum conservation) and energy equations in three dimensions for the fluid for the turbulent flow domain (air).

2.2 Boundary Conditions

Solid and perforated fins cases have been simulated for inlet free stream air velocities of 3, 4, 5, 6, and 7 m/s for the range of Reynolds number(7500-17500) and a temperature of 300K and (0 Pa) relative pressure at outlet for validation of Nusselt number (Nu) and friction factor (f). No slip condition is applied to the outer tube and the fin walls. The inner tube wall was assumed to have a constant temperature of the condensing steam (373 K).The computational domain walls at the tube inlet and outlet are subjected to a symmetrical boundary conditions which is used to reduce computational effort in problem. Free stream air properties were specified as viscosity (μ) $1.798 \cdot 10^{-5}$ kg/m-s Specific heat (C_p) 1006.43 J/kg-K, and thermal conductivity (k) 0.0242 W/m-K, **Banerjee et al, 2012.**

2.3 Mesh Generation

Tetrahedral elements have been used to mesh the flow domain because it is more flexible in representing complex geometry boundaries **FLUENT, 2006.**

A mesh independency test has been carried out by varying the number of elements from 34,560 to 1.7 million. Six types of mesh density have been used to study mesh independence as shown in **Table 2.** Maximum skewness gained in this simulation is 0.75, which indicates that the mesh has suitable quality and would not compromise the solution stability. The meshing of the tunnel and the six circular model are shown in **Fig. 2.**

3. EXPERIMENTAL APPARATUS

The schematic diagram of the test rig is shown in **Fig. 3.** It shows the experimental rig which consists mainly of wind tunnel (duct) have a parallel test section in the middle manufactured from clear acrylic of (300mm x 300mm x 600mm), axial ventilation 3 phase motor (Power =2.2 kW), steam boiler, measurement devices, and steam separator.

The fins are manufactured from thin sheets of copper of thermal conductivity (376W/m. °C). Five dies needed to manufacture the models of heat exchanger. The heat exchangers used in present work have been prepared to be staggered heat exchangers and have equal longitudinal and transverse pitch of tube. The final shape of heat exchanger has been produced by welded the tubes to the U shape elbow. Each one of produced heat exchangers has 144 fins, and 111 cm



total length taken in consideration the equivalent length of elbow. **Fig. 4** shows the final shapes of all models and **Fig. 5** shows the dimensions of heat exchanger. Many thermocouples of type-(K) were used with a digital thermometer having an accuracy of $\pm 0.5\%$ of full scale division for the range of $(0 - 999)^\circ\text{C}$, to measure the temperatures by connecting the thermocouples to digital thermometer in parallel by leads through a selector switch. The thermocouples were distributed within the rig and the heat exchanger to measure the temperature of the air at entry and at exit of the test section, inlet and exit of the heat exchanger. Ten thermocouples were distributed along the fins to measure the temperature in different position on the fin surface. Before the experimental work started and in order to obtain accurate measurements a calibration for the thermocouples, compensating cable, selector switch, and the measuring device were done. Static ellipsoidal nosed pitot tube has been used to measure the static pressure in the tunnel while a portable manometer has been used to measure the differential pressure. A digital anemometer vane-type (model AR826) has been used to measure the average air velocity at entry and exit of the test section. As a different value of air velocity through the duct is required then an inverter used to control fan motor velocity.

3.1 Experimental Procedure

The experiments has been started by operating the steam generator, and waiting till generating steam at 1 bar and 100°C (Saturated steam), then the valve of boiler will open to allow steam flowing continuously inside the heat exchanger until reaching steady state, which represents the starting time of experiments, finally switching (ON) the fan motor to blow air inside the duct through the test section. During each test run, the following data are recorded:

- a- The average surface temperature of heat exchanger ($T_{s,av}$) read from the outputs of the (11) thermocouples distributed in it.
- b- The inlet and outlet air bulk temperature through thermocouple at the entrance and exit section respectively.
- c- The air surrounding temperature, taken by reading room temperature thermocouple.
- d- The new pressure drop (ΔP) between the inlet and outlet will be accurately measured.
- e- Condensation rate of steam.

3.2 Data Analysis

The heat transfer mode in the present work is conduction and convection through the air. The magnitude of each mode depends on the temperature of the fin array base, the geometry and the flow rate. The energy balance is given as

$$\dot{Q}_{condensation} = \dot{Q}_{convection} \quad (1)$$

The latent heat of condensation ($\dot{Q}_{condensation}$) is given by:

$$\dot{Q}_{cond.} = \dot{m}_{cond.} h_{fg} \quad (2)$$

The heat transfer by convection from finned tubes surface including outer surface of tubes is given by:

$$\dot{Q}_{convection} = h_{av} A_s [T_{s,av} - T_{\infty}] \quad (3)$$

where T_{∞} is taken as air inlet temperature

Hence the average convective heat transfer coefficient h_{av} , can be found out as follows:

$$h_{av} = \frac{\dot{Q}_{convection}}{A_s [T_{s,av} - T_{\infty}]} \quad (4)$$

The surface area of all models can be expressed by the following equations:

$$A_s = A_{s \text{ no fin}} + A_{s \text{ fin}} \quad (5)$$

$$A_{s \text{ no fin}} = \pi \times d_r \times P_f \times N_f + A_{s \text{ term}}. \quad (6)$$

$$A_{s \text{ term}} = \pi \times d_r \times 0.006 \quad (7)$$

where 0.006 is the distance between first fin and wall of the duct.

The dimensionless groups, Nusselt number (Nu) and Reynolds number (Re) are calculated as follows:

$$Nu = \frac{h_{av} d_h}{K_{air}} \quad (8)$$

$$Re = \frac{\rho_{air} V_{max} d_h}{\mu_{air}} \quad (9)$$

Hydraulic diameter (d_h) can be expressed as:

$$d_h = (d_f - d_r) \quad (10)$$

The pressure drops over the test section in the model were measured. The pressure drop can be arranged in dimensionless form by using the following relation **Banerjee et al. 2012**.

$$f = \frac{\Delta P}{n\rho_{air}V_{max}^2} \quad (11)$$

ΔP can be expressed as:

$$\Delta P = P_{in} - P_{out} \quad (12)$$

According to the continuity equation, the area of minimum cross section has maximum flow velocity. For finned-tube configurations, the area of minimum cross section is the thin space between the two fins. Hence, the maximum velocity can be calculated from the following equation **Banerjee et al. 2012**.

$$V_{max} = \frac{S_T V}{S_T - dr} \quad (13)$$

Limiting the pressure drop becomes one of the primary challenges in the design of finned-tubes. Perforations, which increase Nusselt number, also increase the pressure drop. Thus the efficiency of perforations is determined to find the optimum case having the least increase in ΔP with the maximum increase in heat transfer per unit area (q). The relative q - ΔP factor is a dimensionless quantity defined as the ratio between heat flux performance ratio and fin ΔP performance ratio **Banerjee et al. 2012**.

$$\text{Fin } q \text{ performance ratio} = \frac{q_{perfo.} - q_{solid}}{q_{solid}} \quad (14)$$

$$\text{Fin } \Delta P \text{ performance ratio} = \frac{\Delta P_{perfo.} - \Delta P_{solid}}{\Delta P_{solid}} \quad (15)$$

$$\text{Relative } q - \Delta P \text{ factor} = \frac{\text{Fin } q \text{ performance ratio}}{\text{Fin } \Delta P \text{ performance ratio}} \quad (16)$$

The Ratio of Heat Dissipation Rate (RQF) is calculated by the relation below:

$$(17)$$

$$RQF = \frac{Q_{perforated\ fin}}{Q_{solid\ fin}}$$

4. RESULTS AND DISCUSSION

4.1 Theoretical part

4.1.1 Velocity Vectors, Pressure Drop and Temperature distribution Contours

Solid and perforated fins were compared in terms of a free stream velocity of 3m/s using velocity vectors and pressure drop contours. **Fig.6** shows projection of the 2-D velocity vectors for fluid flow through solid fins and other perforated models at inlet velocities of 3 m/s. As shown in this figures the free stream air flow approaches the finned-tube array and encounters stagnation at the first row. At this point (stagnation point), the flow velocity is reduced to zero, and the pressure, being inversely proportional to velocity, is the maximum in the domain. Pressure begins to decrease as the flow being enhanced. Maximum velocity is observed at the region between two fins. Thereafter, increasing of pressure and decreasing of velocity lead to creating a positive pressure gradient. This resulted in flow separation from the fin wall, creates wake areas. Fluid particles in this region loss the energy in overcoming the shear forces in the boundary layer.

In the cases of perforated fins, the two perforations in the upstream side will increase the velocity and reduce the pressure, while the other two perforations make a reduction in the wake areas by increasing the velocity too. Comparison of velocity contours shows that perforations alter the velocity gradients in the domain. Moreover **Fig.6** shows that the fluid flow velocities and mixing in perforation cases are more than that in solid case. The cases can be arranged from small to large as solid, four circular, square, triangle, and six circular perforations depending on velocity and mixing of fluid.

Fig.7 show the 2-D pressure contour through solid fins, and other perforated fin models at inlet velocity of 3 m/s. It is clearly shown that the perforated fins have a higher pressure drop than that for solid fins. This increase in pressure drop is due to higher velocities and mixing in perforation cases. The cases can be arranged from small to large as solid, four circular, square, triangle, and six circular perforations depending on pressure drop.

Solid and perforated fins are compared at a free stream velocity of 3m/s using temperature contours. Subsequent to the solid fins, perforations are introduced in the upstream and downstream regions with an attempt to improve the flow characteristics and increase the heat transfer efficiency. Due to the slower air flow, high temperatures persisted in wake areas. Thus, the upstream half of the region experienced higher heat removal than the downstream region. As

the size of recirculation region decreases in case of perforated fin, the high temperature zones in the downstream region decrease due to increase in the mixing and flow rate of air in the downstream areas as clearly shown in **Fig. 8**. Also the temperature contours of the solid and perforated fin shows more reduction in temperature of perforated fin wall. The cases can be arranged from large to small as solid, circular, square, triangle and six circular perforations depending on wall surface temperature and downstream air temperature.

4.1.2 Heat Transfer

Fig. 9 shows the variation of Nusselt number with Reynolds number for all models based on the numerical results. To determine the effect of the Perforations shapes on the amount of heat transfer, a comparison between the (2,3,4) models shows that, triangular perforations model yields the highest Nusselt number while the lowest Nusselt number is observed at the model of the solid fin at all Reynolds numbers in the considered range. This enhancement is due to the bigger width of perforation which faces the flow in case of triangular perforation which causes more destruction or reduction of the area of thermal boundary layer than the other perforation models, and so on for other models. Also it's due to the bigger perforation inner lining surface area which gives more surface area.

The effect of number of perforations on the heat transfer process is determined when comparing between (2 and 5) models in **Fig.9** which shows that the value of Nusselt number for the six circular perforations model (case 5) is higher than that for the model of four circular perforations (case 2) for the same perforation diameter. Increment in the number of perforation will increase the turbulent intensity due to more destruction and abruption in thermal boundary layer, and as a result of increasing of the heat transfer coefficient.

A general comparison among all models taken in the present study, shows that the values of Nusselt number for six circular perforation model is higher than that of the other models due to the reasons which mentioned previously.

4.1.3 Friction Factor (f):

Fig.10 shows that the value of friction factor for the perforated fin is higher than that for solid fin due to increase in pressure drop in case of perforated one because of excessive flow disturbances produced by perforations. It can be noted that the triangular perforations model gives the higher value of pressure drop than that gives by solid fin. The comparison among all

models is shows that the six circular perforations gives the highest value of pressure drop among all models.

Fig. 11 shows the effect of shape and number of perforations on the amount of transferred heat. This may be justified by the net effects of changing heat transfer coefficient and area due to perforations. A higher $q\text{-}\Delta P$ factor value combines the maximum increase in q values in comparison with the minimum increase in ΔP values. Thus, a relative $q\text{-}\Delta P$ factor value greater than unity indicates a better performing fin configuration **Banerjee et al. 2012**. As shown in **Table 3**, the best result for the relative $q\text{-}\Delta P$ factor has been found when the inlet velocities were 6 and 7 (m/s). It is found that the triangle perforation model gives the best result due to excessive increment in the Nusselt number in comparison with pressure drop.

4.2 Experimental Results:

4.2.1 Effect of the Perforations Shapes:

Fig.12 shows the variation of Nusselt number and Reynolds number for solid fin, four circular, square, and triangle perforation models. As shown, there is a good enhancement in heat transfer in the different shapes of different models of perforation. It is clearly shown that the Nusselt number of perforated fins is higher than that of solid case. The cases can be arranged from small to large as solid, circular, square, triangle models depending on the value of Nusselt number. The enhancement of the Nusselt number in each case was (6.52%) in the circular, (8.79%) in the square, and (10.12%) in the triangle model. This was explained previously, because of the bigger width of perforation which faces the flow. The bigger width in case of triangular perforation causes more destruction or reduction in the area of thermal boundary layer more than the other perforation models, and so on for other perforation.

4.2.2 Effect of Number of Perforations:

Fig.13 shows that the Nusselt number for the six circular perforations model is more than that of the model of four circular perforations for the same perforation diameter. The enhancement rate in the Nusselt number was (11.08%) for the six circular perforations model. Increment in the number of perforation will increase the turbulent intensity due to more destruction and abruption in thermal boundary layer, and as a result the heat transfer coefficient.

4.2.3. Friction Factor (f):

Values of pressure drops obtained from the experimental results give comparative results with those observed in the numerical results. **Fig.14** shows the effects of the perforations shapes

on the friction factor. It is clearly shown that the friction factor for the perforated fin is higher than that for solid fin. The greater friction factor refers to increase in pressure drop in case of perforation. In accordance with numerical results, the triangular perforation model causes the highest pressure drop and as a result highest friction factor. Also the effect of number of perforations on the friction factor is shown in **Fig.15** It is easily shown from the figure that the values of friction factor for six circular perforation model is more than the model of four circular perforations

4.2.3. Ratio of Heat Dissipation Rate (RQF):

Fig.16 shows the values of (RQF) calculated from the experimental results which shows a good agreement with that plotted from the numerical results shown in **Fig.11**.As mentioned previously that the shape and number of perforations have effect on the amount of transferred heat.

5. Correlations and Validation

The average Nusselt number for the staggered perforated finned tube heat exchanger were correlated as a function of Reynolds number and the ratio of perforation dimension to fin diameter by using LAB Fit program as followed:

$$Nu = 1.94Re^{0.4286} \left[\frac{d_{eq}}{d_f} \right]^{0.0043} \quad \text{With coefficient of correlation determination (R}^2\text{) of 0.984.}$$

Validation

Fig. 17 and **Fig. 18** shows a comparison between the results of the present numerical study (Nusselt number and friction factor) with the work of **Banerjee et al. 2012**, which gives a similar trend for each other with a observed gap between them which may attributed to the difference in geometrical configuration, dimensions and boundary conditions between the two studies. From **Fig. 19** a good agreement is observed for heat transfer enhancement with maximum deviation of $\pm 10\%$ between the present experimental and numerical results. Also, it is clearly shown from **Fig. 20** that there is a good agreement (with maximum deviation $\pm 13\%$) for the values of friction factor between present experimental and numerical results

6.CONCLUSION

1. The average Nusselt number increases as the number of perforations is increased by a rate depending on the perforation geometry.
- 2.The friction factor increases with perforation due to increase in the pressure drop.



3. Nusselt number of six circular perforation model is about 11.08 % higher than that for solid fin model and with triangular perforation model is about 10.12 % higher than that for the solid fin.
4. Pressure drop of six circular perforations is about 11.15 % higher than that for solid fin model and with triangular perforation model is about 9.79 % higher than that for the solid fin.
5. Triangular perforation heat exchanger model gives the best result from the view of perforation efficiency due to excessive increment in the Nusselt number in comparison with pressure drop.
6. The fin with perforation gives a higher reduction in surface temperature and air temperature in the downstream region than solid fins.

REFERENCES

- Banerjee R. K., Karve M., Ho Ha J., Hwan lee D., and Young I. Cho, 2012, *Evaluation of Enhancement Heat Transfer Within A four Row Finned Tube Array of an Air Cooled Steam Condenser*, Numerical Heat Transfer, Vol. 61, PP. 735-753.
- Fayed I. M., Hussain Y., Abdul Hadi H., and Ibrahim S. H., 2008, *Experimental study of fins perforation effect on thermal performance of helically finned tubes*, Iasj, Vol. 14, PP. 339 - 355.
- FLUENT, 2006, "FLUENT 5 User's Guide "Fluent Inc. Lebanon New Hampshire.
- H.J.Kim, , *A Numerical Analysis for the Cooling Module Related to Automobile Air-conditioning System*, Applied Thermal Engineering, Vol. 28 (2008), PP (1896-1905).
- Incropera F., and Dewitt D., 1996, *Fundamentals of Heat and Mass Transfer*, (4th Edn), Wiley, New York
- Ismail M. F., 2013, *Effects of Perforations on the Thermal and Fluid Dynamic Performance of a Heat Exchanger*, IEEE, Vol. 7, PP. 1178 - 1185.
- Kakac S. , **1981**, *Heat exchangers, thermal hydraulic fundamentals and design*, hemisphere publishing, New York.
- Prasad B. V. S. S. S., and Gupta A. V. S. S. K. S., 1998, *Note on the performance of an optimal straight rectangular fin with a semicircular cut at the tip*, Heat transfer engineering, Vol. 14, No. 1, PP. 239-412.
- R. Karabacak, G. Yakar, 2011 *Forced convection heat transfer and pressure drop for a horizontal cylinder with vertically attached imperforate and perforated circular fins*, Energy Conversion and Management, Vol. 52, PP. 2785–2793.

**NOMENCLATURE**

A_s = surface area m^2

A_{pc} = perforation inner lining surface area m^2

$A_{S\ termin.}$: total surface area between the fins and elbows of the three tubes (m^2)

C_p = specific heat $J/kg.K$

d_{eo} = perforation dimension m

d_f = outer Fins diameter m

d_i = internal Tube diameter m

d_r = external Tube diameter m

d_h = hydraulic diameter m

f = friction factor

h = convective heat transfer coefficient $W/m^2.^\circ K$

h_{fg} = latent heat of evaporation KJ/Kg

k = thermal conductivity $W/m.^\circ K$

\dot{m} = condensation rate Kg/s

N_f = number of fins

N_p = number of perforations

P_f = fin pitch m

Q = heat transfer W

q = heat flux W/m^2

S_T = transverse tube pitch

t = fin thickness m

Greek Symbols

μ = Dynamic viscosity $kg/m.s$

ρ = Variable density kg/m^3

Subscript

av: average

cond.: condensation

term.: terminal

p: perforation

r: root

s: surface

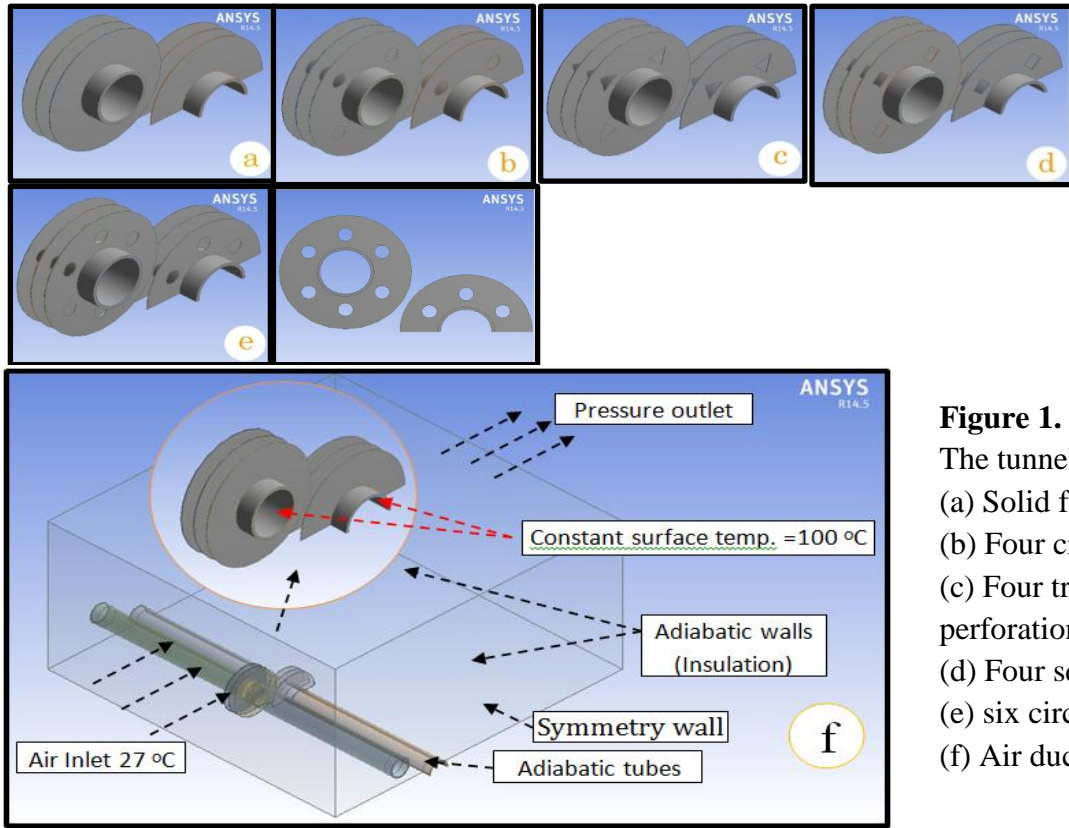


Figure 1.
The tunnel and all cases
(a) Solid fin
(b) Four circular perforation
(c) Four triangular perforation
(d) Four square perforation
(e) six circular perforation
(f) Air duct

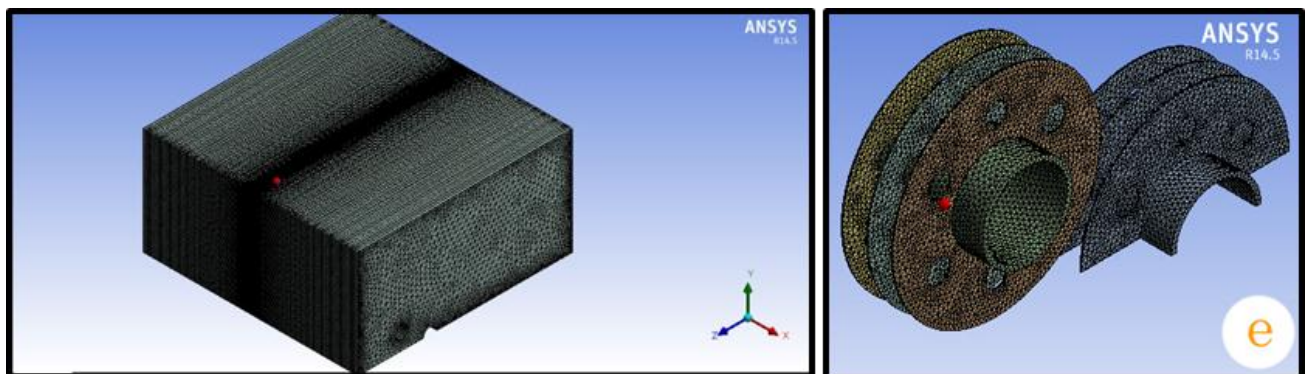


Figure 2. Meshing of tunnel and the six circular model.

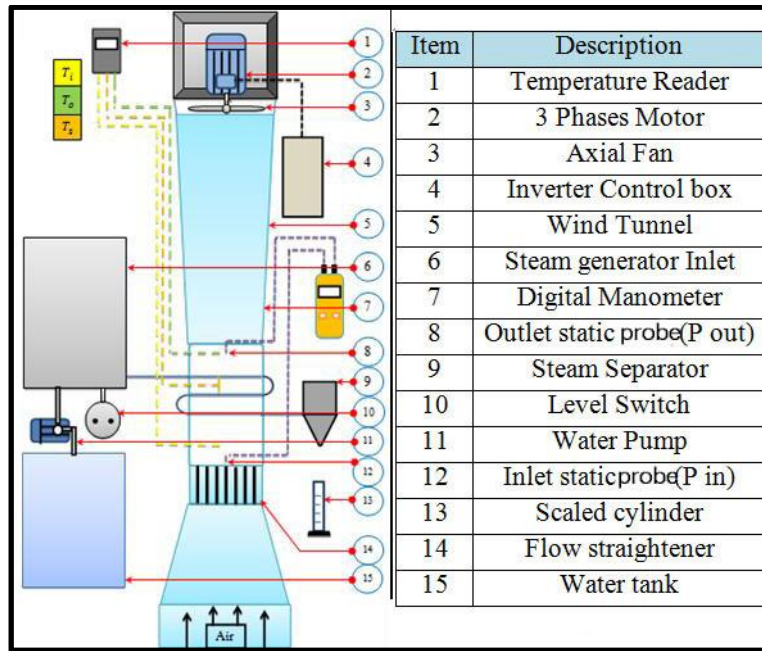
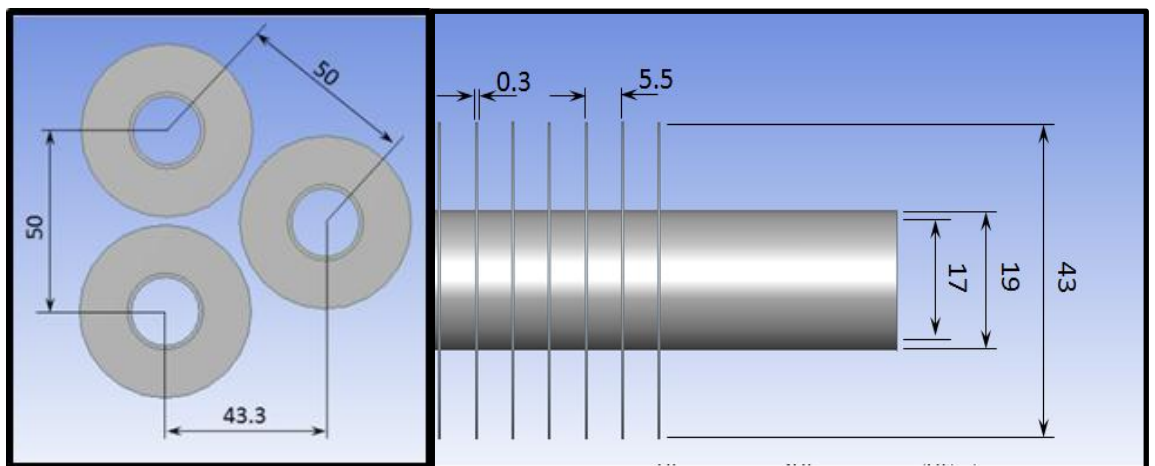


Figure 3. Schematic diagram and photo of the experimental rig.



Figure 4. Experimental models



Figures 5. Dimension of the heat exchanger (in mm)

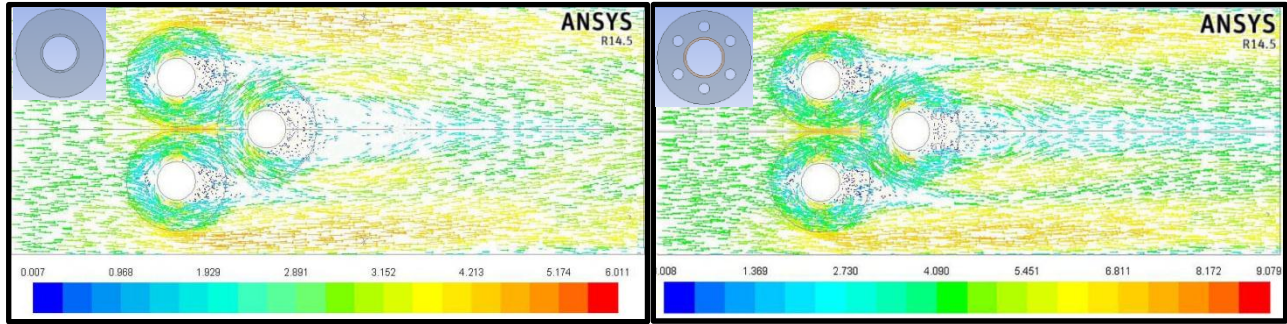


Figure 6. (2-D) Velocity Vector projection for solid and six circular perforation model at 3 m/s inlet velocity

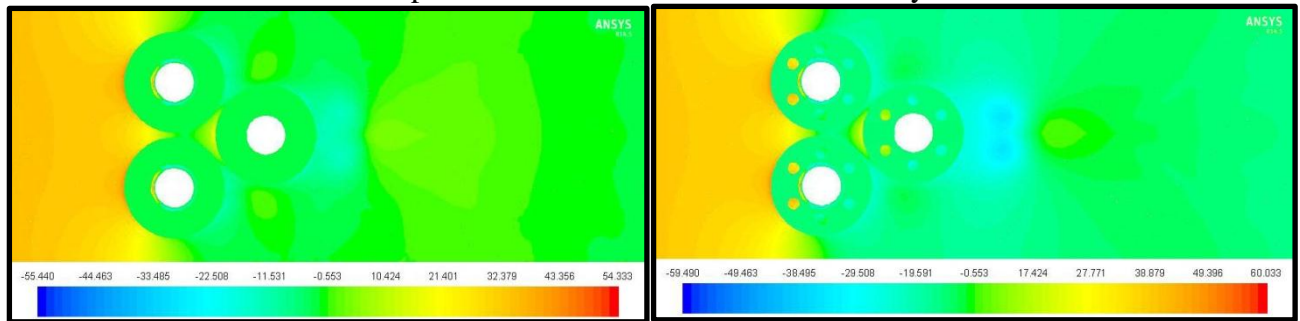


Figure 7. (2-D) static pressure drop projection for solid and six circular perforation model at 3 m/s inlet velocity

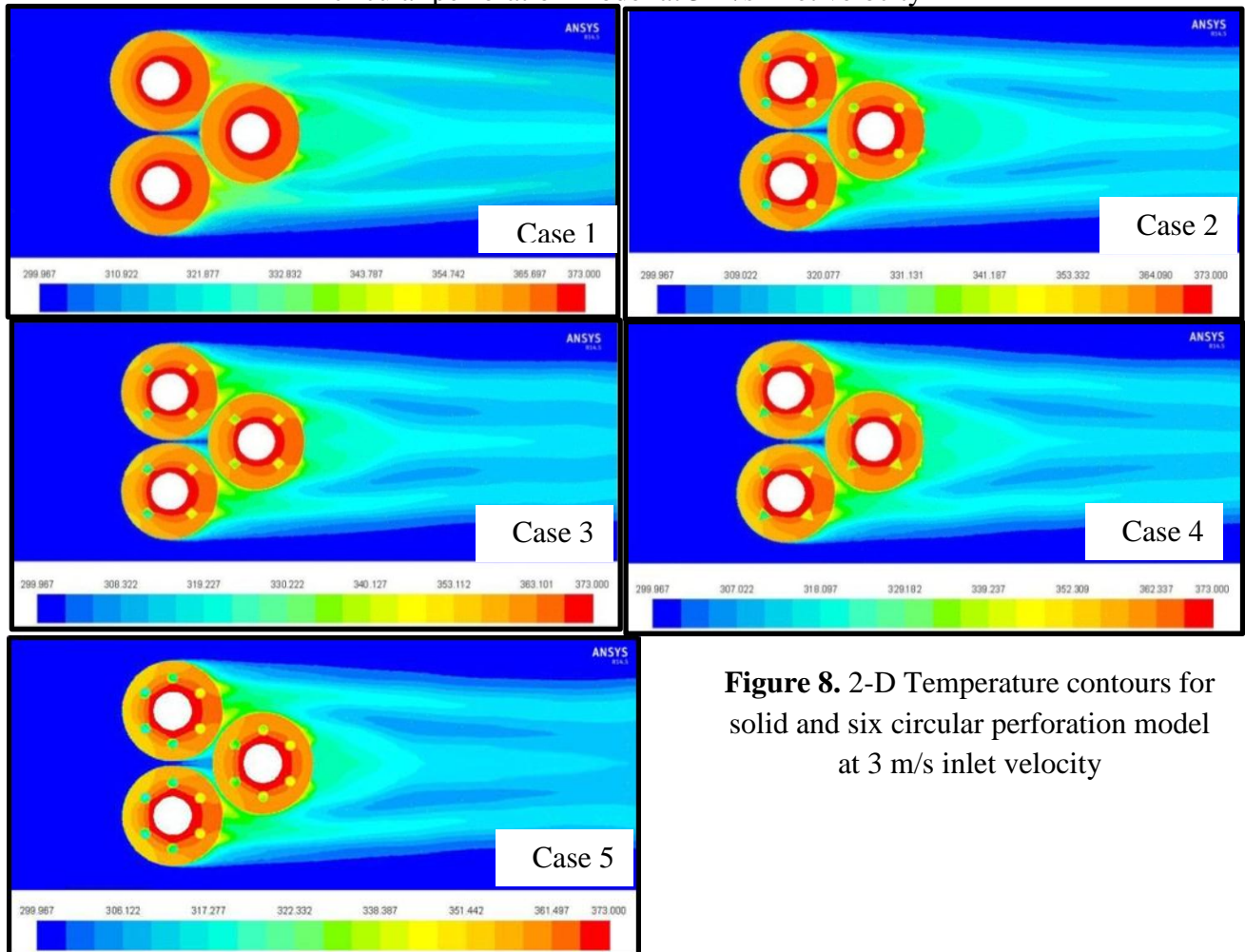


Figure 8. 2-D Temperature contours for solid and six circular perforation model at 3 m/s inlet velocity

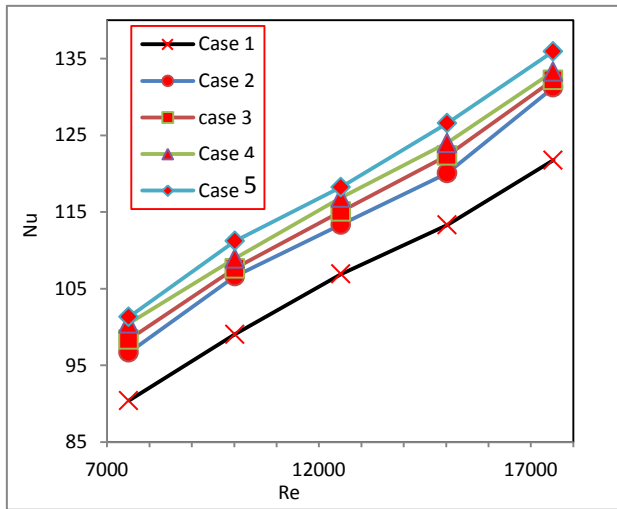


Figure 9. Variation of Nusselt number with Reynolds number for all models based on the numerical results

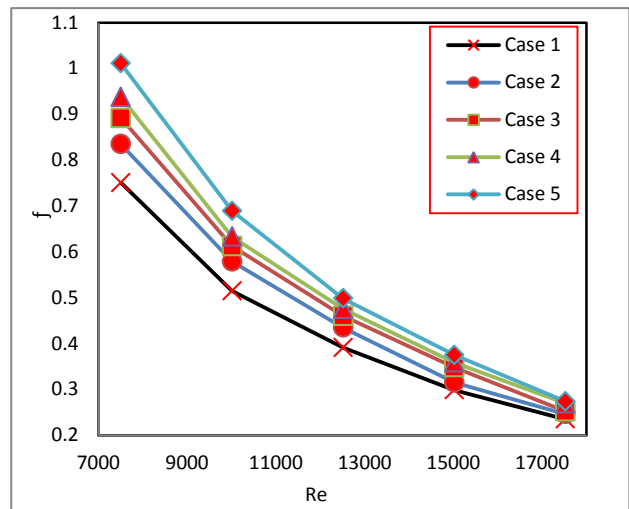


Figure 10. Variation of friction factor with Reynolds number for all models based on the numerical results

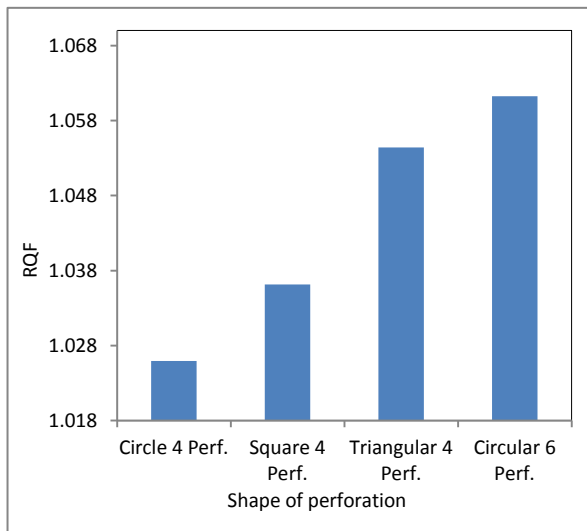


Figure 11. Values of RQF for all models based on the numerical results

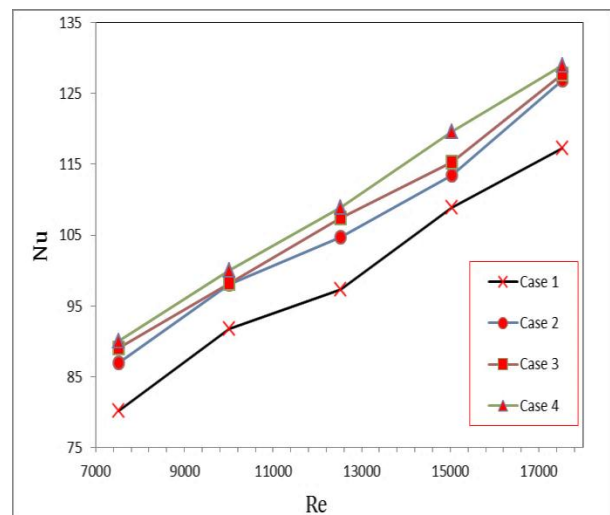


Figure 12. Effect of perforations shape on Nusselt number based on experimental results

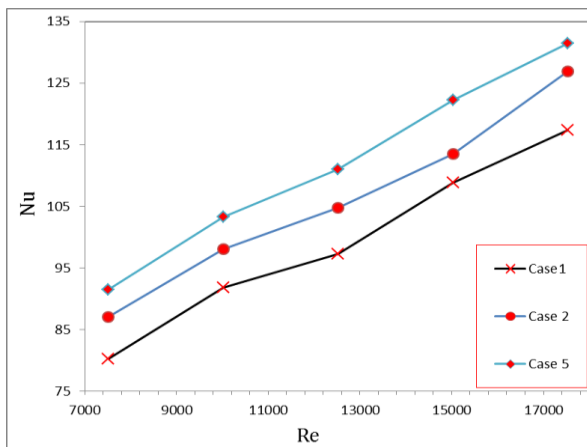


Figure 13. Effect of number perforations on Nusselt number based on experimental results

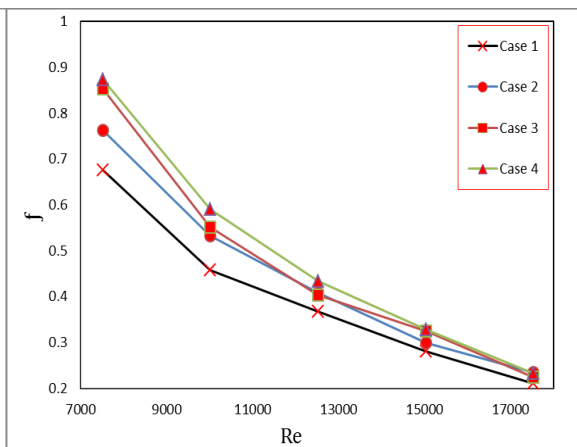


Figure 14. Effect of perforations shape on friction factor based on experimental results

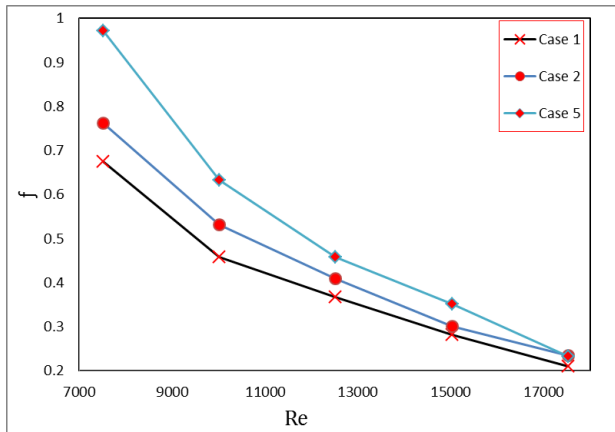


Figure 15. Effect of number of perforations on friction factor based on experimental results

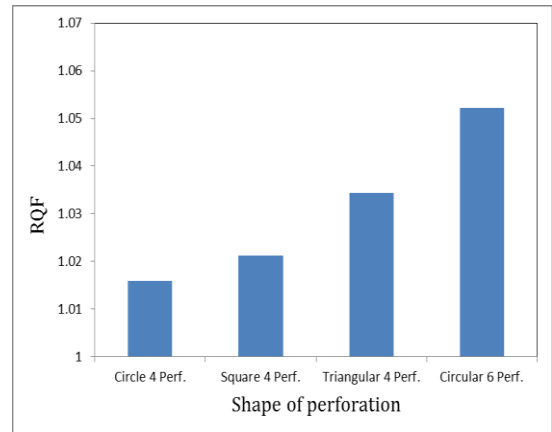


Figure 16. Variation of RQF based on the experimental results

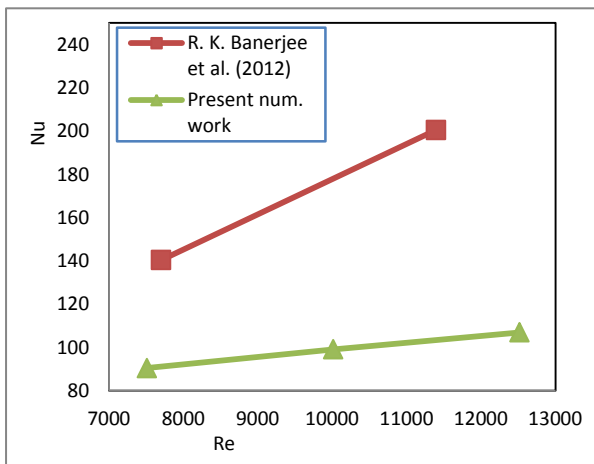


Figure 17. Nusselt number vs. Reynolds number for present numerical results compared with R. K. Banerjee et al.2012

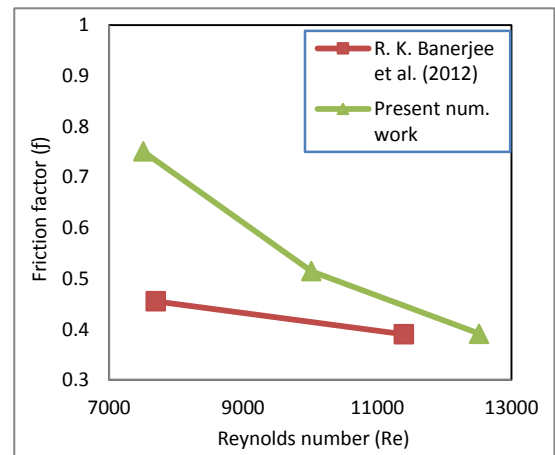


Figure 18. Friction factor vs. Reynolds number for present numerical results compared with R. K. Banerjee et al.2012

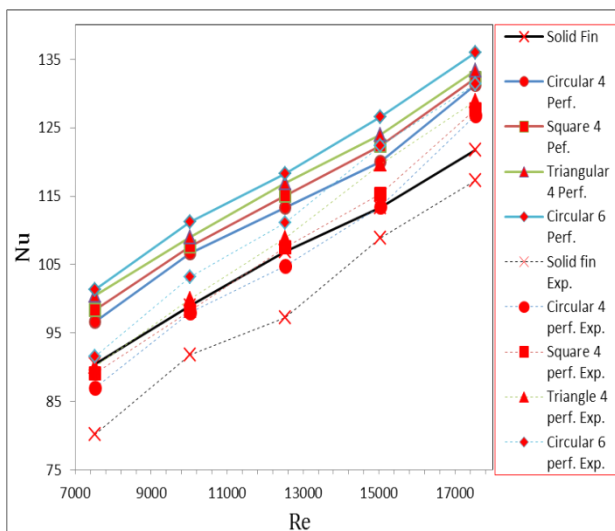


Figure 19. Average Nusselt number vs. Reynolds number for present experimental and numerical results.

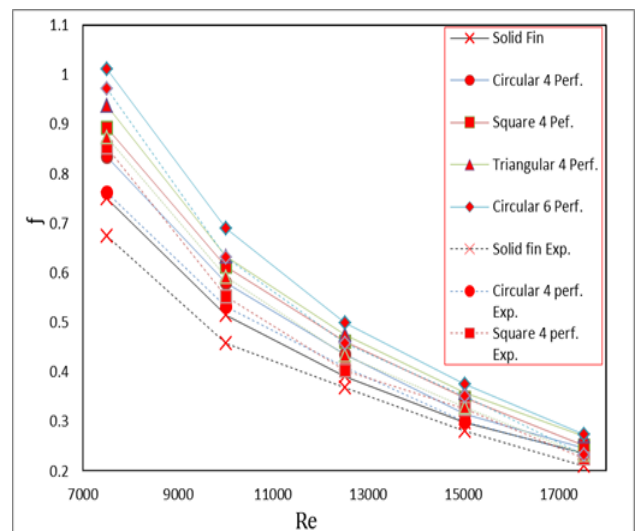


Figure 20. Average friction factor vs. Reynolds number for present experimental and numerical results.



Table 1. Description of the five models.

Cases	Description
Case 1	Solid fin
Case 2	Perforated fin having four circular perforations
Case 3	Perforated fin having four square perforations
Case 4	Perforated fin having four triangle perforations
Case 5	Perforated fin having six circular perforations

Table 2. Mesh dependency results accuracy.

No	Number of elements	Tip temperature(K)	Duct pressure drop (Pa)
a	34560	370.621	61.215
b	103680	369.779	55.747
c	362880	369.173	49.544
d	1200180	368.387	45.651
e	1552460	367.212	44.899
f	1705112	367.105	44.719

Table 3. Relative q-ΔP factor.

<i>Inlet velocities (m/s)</i>	<i>Relative q-ΔP factor</i>			
	<i>Four circular perforations model</i>	<i>Four square perforations model</i>	<i>Four triangular perforation model</i>	<i>Six circular perforations model</i>
3	0.601	0.609	0.697	0.691
4	0.603	0.693	0.801	0.789
5	0.825	0.827	0.892	0.894
6	0.901	0.909	1.095	1.043
7	0.982	1.089	1.213	1.152